Student Research Awards in the Doctoral Degree Candidate Category, 29th Annual Meeting of the Society for Biomaterials, Reno, NV, April 30–May 3, 2003

Use of vascular endothelial cell growth factor gene transfer to enhance implantable sensor function *in vivo*

U. Klueh,[1,2] D. I. Dorsky,[1,3] D. L. Kreutzer,[1,2,4]
[1]*Center for Molecular Tissue Engineering, University of Connecticut, School of Medicine, Farmington, Connecticut 06030*
[2]*Department of Pathology, University of Connecticut, School of Medicine, Farmington, Connecticut 06030*
[3]*Department of Medicine, University of Connecticut, School of Medicine, Farmington, Connecticut 06030*
[4]*Department of Surgery, University of Connecticut, School of Medicine, Farmington, Connecticut 06030*

Received 15 October 2002; revised 21 May 2003; accepted 16 July 2003

Abstract: In the current study, we developed and validated a simple, rapid and safe *in vivo* model to test gene transfer and sensor function *in vivo*. Using the model, we tested the specific hypothesis that *in vivo* gene transfer of angiogenic factors at sites of biosensor implantation would induce neovascularization surrounding the sensor and thereby enhance biosensor function *in vivo*. As the *in vivo* site for testing of our gene transfer cell and biosensor function systems, the developing chorioallantoic membrane (CAM) of the embryo was utilized. Vascular endothelial cell growth factor (VEGF) was used as a prototype for angiogenic factor gene transfer. A helper-independent retroviral vector derived from *Rous sarcoma* virus (RSV), designated RCAS, was used for gene transfer of the murine VEGF (mVEGF) gene (mVEGF:RCAS) into the DF-1 chicken cell line (designated mVEGF:DF-1). Initially, the ability of VEGF:DF-1 cells to produce VEGF and RCAS viral vectors containing the mVEGF gene (mVEGF:RCAS) was validated *in vitro* and *in vivo*, as was the ability of the mVEGF:DF-1 cells to induce neovascularization in the *ex ova* CAM model. Using the system, we determined the ability of mVEGF:DF-1 cells to enhance acetaminophen senor function *in vivo*, by inducing neovascularization at sites of sensor implantation in the *ex ova* CAM model. For these studies, acetaminophen sensors were placed on 8-day-old *ex ova* CAMs, followed by addition of media or cells (mVEGF:DF-1 cells or GFP:DF-1 cells) at the sites of biosensor implantation on the CAM. At 4 to 10 days after sensor placement, the biosensor function was determined by measuring sensor response to an intravenous injection of acetaminophen. Sensors implanted on CAMs with buffer or control cells (GFP:DF-1 cells) displayed no induced neovascularization around the sensor and had minimal/baseline sensor responses to intravenous acetaminophen injection (media, 133.33 ± 27.64 nA; GFP:DF-1, 187.50 ± 55.43 nA). Alternatively, the sensors implanted with mVEGF:DF-1 cells displayed massive neovascularization and equally massive sensor response to intravenous injection of acetaminophen (VEGF:DF-1, 1387.50 ± 276.42 nA). These data clearly demonstrate that enhancing vessel density (i.e., neovascularization) around an implanted sensor dramatically enhances sensor function *in vivo*. J Biomed Mater Res 67A: 1072–1086, 2003

Key words: biosensors; chick embryo chorioallantoic membrane; gene transfer; *in vivo*; neovascularization; Rous sarcoma virus; vascular endothelial cell growth factor

INTRODUCTION

The relatively slow progress seen in the development of implantable sensors is caused in large part by the inability to control the complex tissue responses induced by sensor implantation (i.e., inflammation, fibrosis, and loss of vasculature) and by the lack of a simple, rapid, and cost-effective *in vivo* model to evaluate sensor function and agents that can control tissue reactions to the implanted sensors (e.g., gene transfer or tissue response modifiers). Despite the increasing efforts to develop implantable subcutaneous sensors (e.g., glucose sensors), a reliable long-term continuous monitoring has not been achieved. Generally, the

Correspondence to: D. L. Kreutzer; e-mail: kreutzer@nso2.uchc.edu
Contract grant sponsor: National Institutes of Health, Bethesda, Maryland

main obstacle to the long-term uses of implantable biosensors is loss of sensor function after a relatively short period of time *in vivo*, usually within hours to days following implantation. This loss of sensor function is believed to be due to the tissue reaction triad (TRT) of inflammation, fibrosis, and vessel regression.[1–6] Prior efforts to overcome the loss of sensor function associated with the TRT usually depended on the uses of "stealth coatings" to "hide" the implanted sensors from tissue reactions induced *in vivo*. Unfortunately, the approaches met with little success. We have chosen an alternative approach to the "stealth technology," that is, the use of tissue response modifiers (TRMs) such as drugs, genes, and matrices to directly control the TRT at sites of sensor implantation. We hypothesize that directly controlling TRT at site of sensor implantation, with tissue response modifiers, will enhance sensor function and lifetime *in vivo*. However, suppressing inflammation and fibrosis using TRMs to control tissue reactions and enhance sensor function is a challenging approach, because these are extremely powerful tissue reactions. One alternative approach to enhancing sensor function *in vivo* would be the induction of new blood vessel formation in the tissue surrounding the sensor using angiogenic factor gene transfer technology.

In light of recent advances in the use of the angiogenic factor vascular endothelial cell growth factor (VEGF) gene transfer to induce new vessel formation in injured and ischemic tissue, for example, heart tissue[7–13] and the critical role of blood vessels in sensor function *in vivo*, we hypothesized that: (1) local tissue transfection of VEGF genes with associated local expression of VEGF, would increase new blood vessel number and density around implanted sensors *in vivo*; and (2) this VEGF-induced increase in vessel number, density, and blood flow will enhance sensor function *in vivo*. To test this hypothesis and provide "proof of principle" that gene transfer induced neovascularization can enhance sensor function *in vivo* we developed the following model systems. The *in vivo* model selected for the studies was the *ex ova* chorioallantoic membrane (CAM) model because of its simplicity and speed for testing *in vivo* responses.[14–18] For these studies, VEGF was selected as our prototype angiogenic factor for gene transfer. The selection of VEGF was made because, unlike many other angiogenic factors, VEGF does not activate fibroblasts.[19–22] To deliver murine VEGF (mVEGF) gene, a helper-independent retroviral vector derived from Rous sarcoma virus (RSV), designated RCAS, was used to introduce the mVEGF gene into DF-1 chicken cells *in vitro*. Although the RCAS vector is replication-competent, it is also transformation-defective, because the *sarc* gene has been deleted.[23] Therefore, no transformed foci (sarcomas) develop in the CAM due to the vector. In addition, the vector system is easily manipulated by standard recombinant DNA methods, replicates robustly in DF-1 avian cells *in vitro*, and does not infect mammalian cells which provides an added safety feature.[24,25] To determine whether this VEGF-induced neovascularization would enhance sensor function *in vivo*, we utilized an acetaminophen sensor. The acetaminophen sensor system was selected because of its simple design and the fact that acetaminophen is not found in chicken blood, thus simplifying data analysis and interpretation.

Using the mVEGF:RCAS viral vector, we successfully constructed and validated the mVEGF:DF-1 cells for mVEGF:RCAS and mVEGF protein expression *in vitro*. Using the mVEGF:DF-1 cells, we successfully induced neovascularization in the *ex ova* CAM model. When the VEGF:DF-1 cell system was implanted with the acetaminophen sensor in the *ex ova* CAM, the mVEGF:DF-1 cell systems were able to induce robust neovascularization in the animal model and dramatically enhance sensor function *in vivo*. The studies provide the foundations for future studies of not only the impact of gene transfer–induced neovascularization on sensor function *in vivo* but *in vivo* studies of the impact of a wide variety of genes on tissue reactions and implant function *in vivo*. Thus, our recently developed *ex ova* model of the chick embryo,[14] coupled with cell-viral vector–based gene transfer system, should provide the new tools and paradigms needed to rapidly advance the development of implantable sensors but of implants in general.

MATERIALS AND METHODS

Cell culture

The chicken fibroblast cell line DF-1[26,27] was obtained from Drs. Rowe and Lichtler (University of Connecticut Health Center, Farmington, CT). Growth medium consisted of Dulbecco's modified Eagle medium supplemented with 5% fetal calf serum, 5% bovine calf serum, 10% tryptose phosphate broth, streptomycin (100 U/mL), penicillin (100 U/mL), and amphotericin B (Fungizone, 2.5 μg/mL). Cells were cultured at 37°C in a humidified atmosphere of air containing 5% CO_2. Additionally, cultures were supplemented with 8 μg/mL of hexadimethrine bromide (Polybrene; Sigma Chemical Co., St. Louis, MO).

Rous sarcoma virus vector model of gene transfer

A helper-independent retroviral vector, RCAS, derived from RSV was used for gene transfer in the *in vitro* and *ex ova* CAM model studies.[28] The mouse murine VEGF gene (mVEGF) was inserted into the RCAS proviral plasmid vector in both "sense" and "antisense" orientations using stan-

dard recombinant DNA manipulations.[29] Specifically, a 908-bp Taq I fragment containing the mVEGF open reading frame was mobilized from pBSK+mVEGF (obtained from Dr. Kevin Claffey, University of Connecticut Health Center) and ligated into the unique Cla I site of the RCAS-BP(A) proviral vector plasmid. The ligation products were screened by restriction mapping, and both sense and antisense orientations were obtained. The resulting mVEGF and anti-mVEGF proviral DNAs were transfected into DF-1 chicken fibroblast cells using lipofectamine, and the cultures were passaged for 2 weeks to allow viral replication. The RCAS-EGFP (enhanced green fluorescence protein) used in the studies was obtained from Dr. Lichtler, University of Connecticut Health Center.

Enzyme-linked immunospecific assays (ELISA)

Expression of mVEGF164 protein was measured with ELISA using a mouse VEGF specific antibody (Ab) and standard curve developed using mVEGF164 protein (R&D System, Minneapolis, MN). The lower limit of sensitivity of the mVEGF ELISA was ≈8 pg/mL. Expression of p27, an RCAS avian leukosis viral protein, was measured by ELISA using a rabbit anti-p27 IgG antibody and a p27 antigen standard provided by SPAFAS (Storrs, CT). Next, a standard curve was prepared in which the levels of p27 antigen were expressed as dilutions, with the lowest detectable dilution being 1/3600.

Evaluation of mouse mVEGF protein expression and RCAS avian leukosis (p27) protein expression after viral infection

To determine and correlate mVEGF protein and RCAS viral production over a 1-week period, the various infected DF-1 cells were seeded at low confluence and monitored for their products until they reached confluence. For that, DF-1 cells and DF-1 cells previously infected with RCAS carrying gene for mVEGF, antisense-mVEGF (AS-mVEGF) or EGFP were seeded in triplicate in 12-well plates at 1×10^4 cells/well. The following days, an aliquot of the culture medium was taken out and replaced by fresh serum containing media. Aliquots were stored at −70°C until evaluated for mVEGF and p27 expression. Protein expression of mVEGF and p27 were measured by ELISA as described above.

Preparation of *ex ova* model of the chick embryo

Fertilized chicken eggs (white leghorn strain) were obtained from the University of Connecticut Poultry Farm (Storrs, CT) and cultivated in petri dishes as previously described.[14]

Evaluation of the tissue reactions and mVEGF expression in the *ex ova* model of the CAM

Gross evaluation

To evaluate and document any viral/gene effects on viability or gross morphological changes induced in the CAM, mVEGF:DF-1cells, various DF-1 control cells, media only, or nylon alone was implanted on the CAMs. The resulting CAMs were examined at various times postplacement (PP) of the test material, using a Zeiss stereomicroscope. The gross morphology of tissue reactions to the various test materials was documented with a SPOT camera (Diagnostic Instruments, Inc., St. Sterling Heights, Michigan). In parallel studies, nontreated chick embryo CAMs were also evaluated for gross morphology and documented as described above for the various cell systems. Generally for these studies, evaluation of gross appearance of test and control CAMs were done at 4 days, 6 days, and 8 days PP of the test material on the CAM.

Histological evaluation

For histological evaluation of tissue reactions induced in the CAMs, controls, or the nylon fabrics (with or without DF-1 cells), treated CAMs were fixed *in situ* (4% buffered formaldehyde) at various days postplacement of the test sample on the CAMs. The fixed tissue was then processed for paraffin embedding and sectioning as previously described.[30,31] Generally, 5-μm sections were prepared of the various specimens, mounted on glass slides, and stained with hematoxylin and eosin (H&E) for evaluation of histopathology.

mVEGF expression *in vivo*

Although our *in vitro* studies demonstrated that the mVEGF:DF-1 cells produced mVEGF, we believe that it is important to demonstrate *in vivo* expression of mVEGF in our CAM model. For these studies, media, mVEGF:DF-1 cells or control cells (DF-1, GFP:DF-1 and mVEGF antisense: DF-1 cells) or media were placed onto the CAM and into a nylon ring. At day 8 postimplantation, the nylon rings were removed from the CAMs and the nylon ring–associated CAM tissue was removed and homogenized using a glass homogenizer and a 0.1% triton phosphate-buffered saline (PBS) buffer to enhance protein extraction. The resulting homogenates were clarified by centrifugation, assayed for mVEGF content by ELISA (R&D Laboratories; also see details of ELISA assay above) and for protein content by BCA protein assay (Pierce Chemical Company). All CAM data was normalized by calculation of picograms of mVEGF per milligram of total protein.

Genetically engineered cell systems for delivery of genes in the *ex ova* model

Several studies suggest that *in vivo* production of heterologous proteins is often most efficient when the tissue site is

implanted with engineered factor-producing cells rather than viral vectors alone.[32–35] Additionally, in bioengineering applications, it would be desirable to mark the tissue site at which the factor production occurs. To address these issues, we utilized a nylon fabric (mesh 35 and 1-μm pore size, Sefar America Inc., Depew, NY) as both a cell carrier system, as well as a marker system, to track the site of cell transfer onto the CAM. Specifically, for the cell carrier system, the nylon fabric was cut in 7-mm disks, ethylene oxide–sterilized, dip-coated in sterile egg white, and placed into a tissue culture–treated 48-well plate and manifested with an o-ring. We utilized DF-1 chicken fibroblast infected with RCAS carrying gene for mVEGF, RCAS carrying gene for antisense to mVEGF, and RCAS carrying gene for EGFP. We also utilized DF-1 chicken fibroblast only as an additional control. Confluent monolayers were gently washed with PBS, pH 7.2, and after a short exposure to trypsin, the cells were suspended in serum containing media. The cell suspension was counted in a hemocytometer and diluted with cell culture medium to a final concentration of 5×10^5 cells/mL. A 100-μL aliquot of that cell suspension was added to the nylon fabric disk and the cells were allowed to grow on the nylon for 2 days prior to placement onto the CAM. The nylon fabric disks were then gently dipped into PBS prior to placement onto the CAMs of 8-day-old chick embryos. After 4, 6, and 8 days PP of the nylon fabric disks, the CAMs were fixed *in situ* and the resulting specimens were processed as described above for evaluation of gross morphology and histology.

Because growing cells on the nylon fabrics was time- and labor-intensive, we investigated the alternative approach of adding the various cell lines directly onto the CAM. For these studies we utilized nylon fabric cut into rings, with an inner diameter of 7 mm, as a marker for the cell application site on the CAM. Confluent monolayers of the various cell lines were washed, trypsinized, and resuspended in serum containing media to a final cell concentration of 1.5×10^6 cells/mL and 50 μL of that cell suspension was directly added into the nylon ring. Additionally, the nylon ring was dip-coated in egg white prior to placement onto the CAM. After 5 and 8 days post-placement of the nylon rings, the CAMs were fixed *in situ* and the resulting specimens were processed as described above for evaluation of gross morphology and histology.

Sensor fabrication

Sensor fabrication was performed utilizing established protocols with modifications.[36,37] Briefly, the acetaminophen sensor consisting of a Teflon-coated platinum (Pt) wire (Medwire, Mt. Vernon, NY) was coiled around a 13-G needle after the Teflon had been removed at its extremities. The coiling area served as the working electrode for our acetaminophen sensor. The coiled Pt wire was then anodized at 1.9 V and cycled between −0.26 and +1.1 V versus a saturated calomel electrode and with a Pt wire (Alfa Aesar, Ward Hill, MA) counter electrode in 0.5*M* H_2SO_4 utilizing a CV-27 potentiostat (Bioanalytical Systems, West Lafayette, IN). Next, electrodeposition of a poly(o-phenylenediamine) (PPD) (Sigma Chemical Co.) film was conducted at +0.65 V for 10 min. The sensor was dried for 0.5 h at room temperature before dip-coating the sensors with six layers of Nafion (Sigma Chemical Co.). Sensors were cured for 0.5 h at 120°C and stored dry at room temperature in closed containers. Nafion coating and PPD film formation were utilized because they are known to prevent biosensor fouling.[38,39]

Sensor function *in vitro*

The acetaminophen sensor (working electrode) was characterized in pH 7.4 PBS at 0.7 V versus a small reference electrode (World Precision Instruments, Sarasota, FL) and utilizing a Pt foil as the counter electrode. The background current was allowed to stabilize for about 20 to 30 min, and increasing amounts of acetaminophen solution (Sigma Chemical Co.) were added to examine sensitivity and linearity.

Sensor function *in vivo*

Sensor-cell placement on *ex ova* CAM

After sterilizing the sensors by overnight UV exposure, sensors were dip-coated in egg white (EW) to enhance cell attachment. The sensors were placed into a 60×15-mm tissue culture–treated petri dish and after the EW was dried out, a fibrin clot containing either media or the cell suspensions (mVEGF:DF-1 or GFP:DF-1) was formed on top of the sensor loop. The formation of fibrin clots served as a matrix to keep the cells localized around the sensor. Briefly, equal amounts of human fibrinogen (6 mg/mL; Sigma Chemical Co.) and cell suspension (2 million cells/mL) or media were mixed and a 50-μL aliquot was placed onto the sensor loop. Five microliters of a 2.5E-3 U/μL thrombin solution (Sigma Chemical Co) was added directly onto the fibrinogen/cell or fibrinogen/media mixture. Polymerization was complete within 15 min at 37°C and produced a three-dimensional gel of fibrin entrapping cells and sensor or culture media and sensor. Sensors were lifted out of the petri dish, and care was taken to make sure most of the fibrin clot entrapping the cells was still attached to the sensor. The sensor was then placed on top of the CAM of an 8-day-old chicken embryo.

Evaluation of sensor function *in vivo*

Sensor performance *in vivo* was conducted 6 to 10 days PP of the sensor using the three-electrode system described above. The petri dish containing the developing chicken embryo was placed into a sand box, which was kept at 38°C and a potential of 700 mV was applied to the working electrode. After stabilization of the background current, 200 μL of a 50-m*M* acetaminophen solution (in PBS) was injected intravenously, and the sensitivity to acetaminophen was determined and recorded onto a chart recorder (Bioanalytical Systems). The sensor current was monitored for approximately 20 min before another intravenous injection of

Figure 1. Morphology of control and RCAS-infected DF-1 cells. The various RCAS viral vectors have no effect on DF-1 cell viability or morphology [i.e., GFP:DF-1, antisense:DF-1(AS-mVEGF:DF-1), or mVEGF:DF-1 cells] [Fig. 1(B–D)] when compared with non–RCAS-infected DF-1 cells [Fig. 1(A)]. Figure 1(E) is the fluorescence picture to Figure 1(D). [Color figure can be viewed in the online issue, which is available at www.interscience.wiley.com.]

acetaminophen was performed. Sensor response to acetaminophen was calculated as nano Amperes (nA) of the initial current increase.

Statistical analysis

All *in vitro* and *in vivo* data obtained for these studies is expressed as mean ± standard deviation. *In vitro* mVEGF data is expressed as picograms of mVEGF per milliter of tissue culture media (pg/mL), and for sensor response *in vitro* and *in vivo* the data is expressed as nano Amperes (nA). Statistical significance for all data was determined using the Student's *t*-test with statistical significance achieved at $p \leq 0.05$.

RESULTS

Rous sarcoma virus vector model of gene transfer

We initially evaluated the *in vitro* impact of the RCAS viral vector on viability and morphology of the chicken DF-1 cell line. The RSV-derived RCAS vector efficiently infected DF-1 chicken fibroblasts and CAMs and is easy to construct and propagate (see below). Figure 1 demonstrates that no effect on DF-1 cell viability and morphology was noted for any of the RCAS vectors used in these studies. The successful infection of the DF-1 cells was directly demonstrated using the GFP RCAS virus, which transformed the nonfluorescent DF-1 cells into fluorescent cells [Fig. 1(D,E)]. Additionally, the presence of the RCAS virus in DF-1 cell cultures was demonstrated by immunocytochemistry using an antibody to the Rous sarcoma virus p27 *gag* gene product (data not shown) as well as soluble p27 viral coat protein (see below).

In vitro evaluation of MVEGF protein expression and avian leukosis p27 protein expression after viral infection

Once we established that the viral infection did not impact cell viability or morphology [Fig. 1(A–E)], we next determined the virus and mVEGF expression in the DF-1 cell lines. For these studies, we measured p27 antigen (a marker of virus content/production by cells) and mVEGF production by ELISA from the control DF-1 cells as well as the viral transfected cells using ELISA technology (Fig. 2). As expected, all cell lines, except the noninfected parental DF-1 cells, produced significant amounts of p27 antigen [Fig. 2(A); data not shown for DF-1, GFP:DF-1, AS-mVEGF:DF-1]. The mVEGF production was detected only from

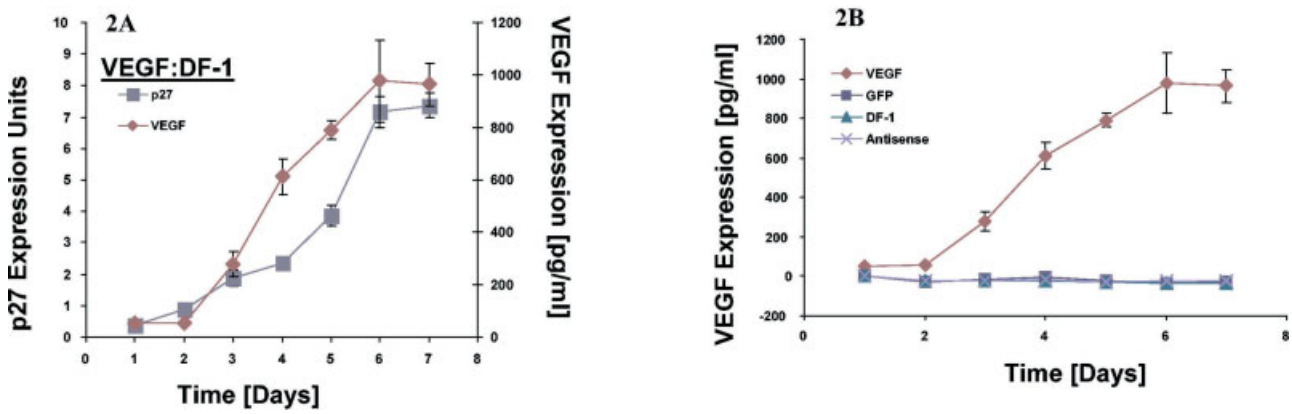

Figure 2. *In vitro* expression of p27 and mVEGF in control and RCAS-infected DF-1 cells *in vitro*. [Color figure can be viewed in the online issue, which is available at www.interscience.wiley.com.]

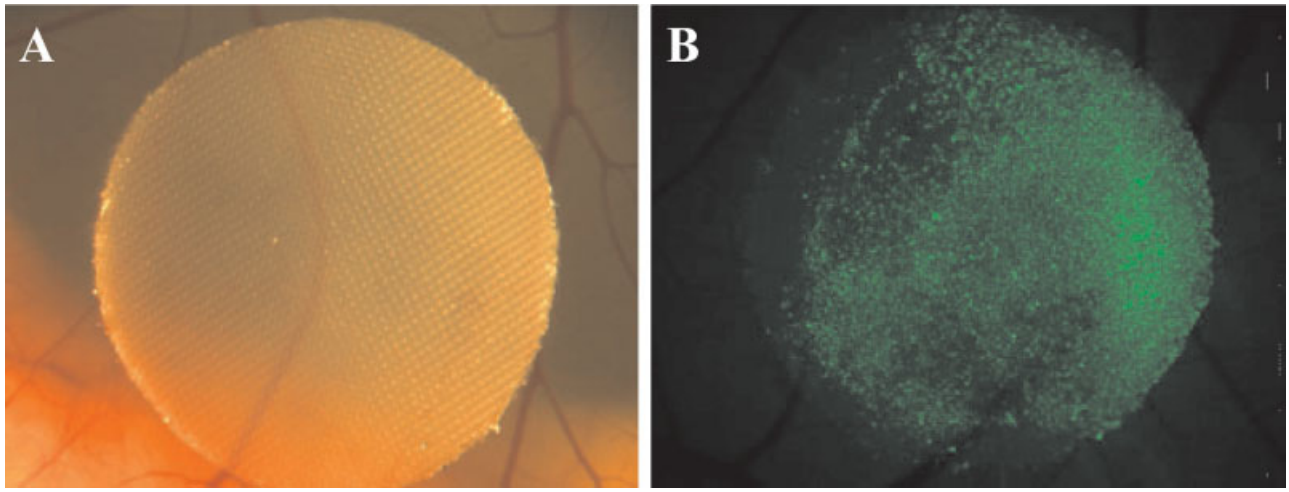

Figure 3. Gross morphologic appearance of GFP:DF-1 cells on nylon disks on CAM (at time point 0). Figure 3(A) demonstrates the bright-field image of GFP:DF-1 cells grown on nylon disks and placed onto the CAM at time point 0. Figure 3(B) demonstrates the fluorescent image of GFP:DF-1 cells at time point 0 as the representing cell line to show the ability of DF-1 cells to grow on nylon fabric. [Color figure can be viewed in the online issue, which is available at www.interscience.wiley.com.]

RCAS-mVEGF–transfected DF-1 cells [Fig. 2(A,B)]. The peak mVEGF production by the mVEGF:DF-1 cells *in vitro* was 978 ± 155 pg mVEGF/mL. A time study of p27 and mVEGF expression in RCAS-mVEGF–transfected DF-1 cells [subconfluent to confluent; Fig. 2(A)] indicated that both p27 and mVEGF production peaked at day 6 in culture (i.e., 80% confluent cells). Thus, our ELISA data clearly indicate that we can infect DF-1 cells with *Rous Sarcoma* Virus (anti-p27) and transfect mVEGF into these DF-1 cells and that these transfected cells clearly produce both RCAS virus and mVEGF.

Genetically engineered cell systems for delivery of angiogenic factors

To maximize mVEGF:DF-1 cell delivery/mVEGF expression to the CAMs, as well as directly mark the tissue site of cell implantation, we utilized a nylon fabric as both a cell carrier/support system, as well as a marker system, to track the site of cell transfer onto the CAM. For these studies we used DF-1 cells and DF-1 cells engineered by gene transfer, and either: 1) grew the cells on small circles of nylon fabric ("Disks") and transferred those to the *ex ova* CAM membrane; or 2) prepared small pieces of nylon fabric with holes in the center ("Rings") to which cells were added directly after placement of the nylon ring on the CAM. Figure 3(A) demonstrates the bright-field image of GFP:DF-1 cells grown on nylon disks and placed onto the CAM at time point 0. Figure 3(B) demonstrates the fluorescent image of GFP:DF-1 cells as the representing cell line to show the ability of DF-1 cells to grow on nylon fabric. This study demonstrated that the DF-1 cell line is able to grow on the nylon fabric. Figure 4 demonstrates the ability of the GFP:DF-1 cells grown on the nylon disks to infect the CAM tissue. It appears by comparing the bright-field images of the gross pictures [Fig. 4(A–C)] with the matching fluorescent images of the nylon disks [Fig. 4(E–G)] that only the CAM tissue growing on top of the nylon fabric is infected and as such expresses GFP. The fluorescent ring seen in GFP:DF-1 nylon fabrics is a result of cells accumulating at the edge of the inner ring [Fig. 4(H)]. Figure 4(D) is the matching bright-field image to Figure 4(H). Figure 4(I–L) demonstrates the histology (H&E) of the nylon disks at time points 4, 6, and 8 days post-placement (PP) and nylon rings at day 8 PP. No histological abnormality could be detected for any of the various time points.

mVEGF-induced neovascularization of CAM

The effect of mVEGF expression in our *ex ova* CAM model was investigated by placing mVEGF:DF-1 cells directly on the CAM. As can be seen in the gross pictures of Figure 5(B–D), the use of nylon disks containing mVEGF-secreting DF-1 cells resulted in a massive growth of vessels within the nylon fabric, which can be seen as early as 4 days PP. On day 4 PP, an increase in the number of blood vessels in the stroma surrounding the ectoderm was seen histologically [Fig. 5(F)]. The expansion of the vasculature continued rapidly and by day 6 PP, parts of the entire stroma were covered with capillaries [Fig. 5(G)]. By day 8 PP, the entire stroma was filled with capillaries, pushing the nylon fabric toward

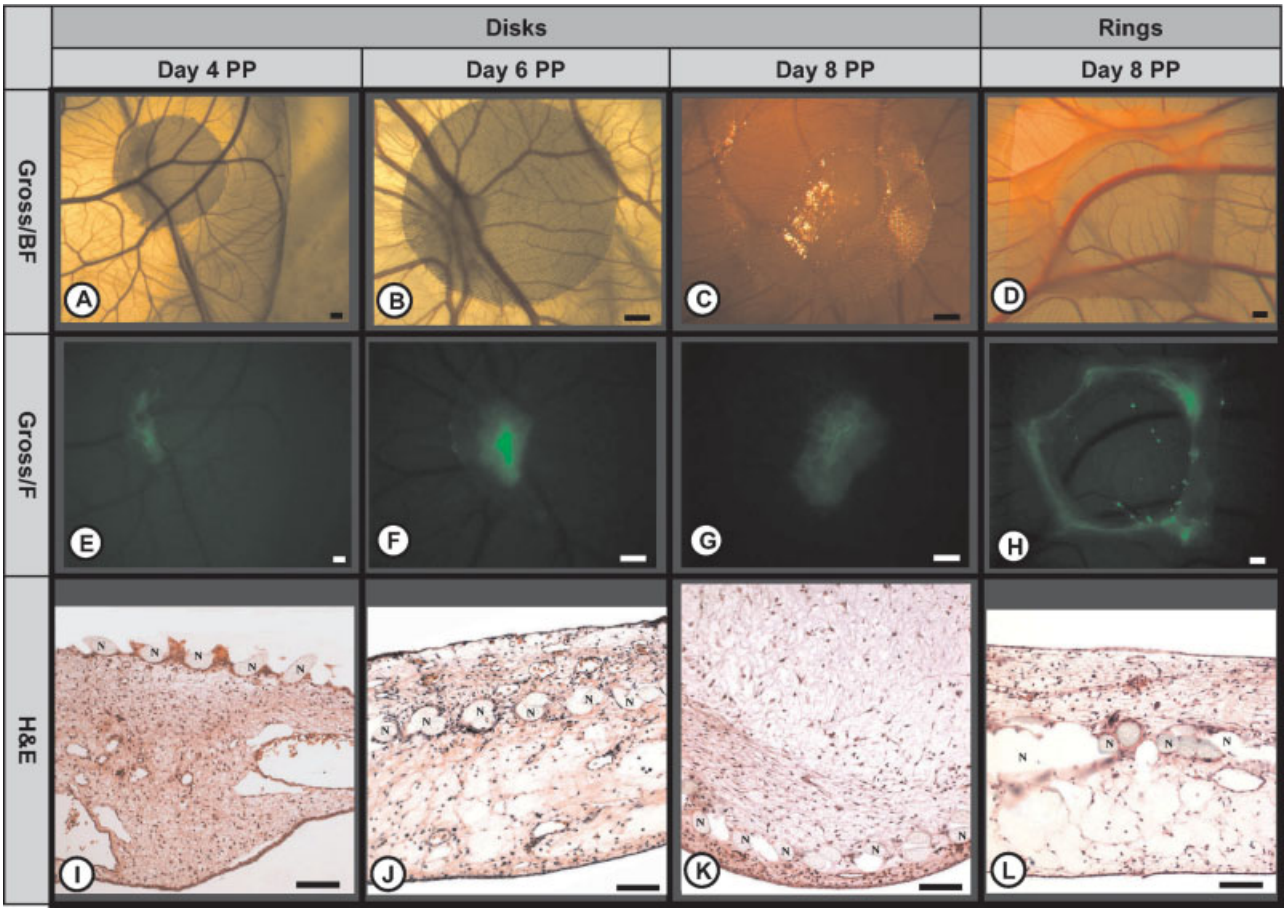

Figure 4. Gross morphologic and histologic appearance of GFP:DF-1 cells growing on nylon disks or placed in nylon rings on CAMs. The nylon mesh appears histologically as gray circles or "empty holes" in the tissue and is marked with the letter N for easy identification in the photographs of the histological sections [Fig. 4(I–L)]. Bar size for gross pictures represents 1 mm. Bar size for histology pictures represents 100 μm. [Color figure can be viewed in the online issue, which is available at www.interscience.wiley.com.]

the endoderm [Fig. 5(H)]. It should be noted that unlike mammalian red blood cells, avian red blood cells are nucleated and, thus, can be mistaken for leukocytes.[14,40] As controls for these studies, we added uninfected DF-1, AS-mVEGF, or RCAS-GFP–infected DF-1 cells to the CAMs. None of the control cells caused significant increase in blood vessel formation in the CAM. We also utilized "nylon-only" (i.e., nylon disks without any cells) controls on the CAMs, which also did not induce new blood vessel formation. See Figure 5(A) for a gross appearance of control CAMs and Figure 5(A) for a histology of control CAMs. It should be noted that the empty spaces in the histological sections are where nylon fabric fibers [designated as "N" in Fig. 5(C–H)] fell out of the tissue sections. Interestingly, the cell addition to the nylon rings utilizing the RCAS-mVEGF construct showed a ring of neovascularization at the edge of the inner circle, which is a result of cells accumulating at the edge of the inner circle, as demonstrated earlier by the use of GFP:DF-1 cells [Fig. 6(B)]. In contrast, control cell addition failed to induce neovascularization [Fig. 6(A)]. Figure 6(C,D) shows the histology of the nylon rings. As can be seen, an intensive capillary development is the case for the mVEGF:DF-1 cells but not for the control. Figure 7 represents a higher magnification of the histology of normal CAMs [Fig. 7(A)] and mVEGF:DF-1/ [Fig. 7(B)] implanted CAMs on day 8 PP. As can be seen in Figure 7(B), the mVEGF:DF-1 cells induce massive neovascularization in the stroma of the CAMs, that is, numerous vessels containing nucleated red blood cells within the lumen of the vessels. As mentioned earlier, avian red blood cells are nucleated cells with red cytoplasm and should not be confused with leukocytes. Thus, we have established a simple, safe, and efficient viral vector–cell delivery system for gene transfer in our *ex ova* CAM model. Finally, these data clearly demonstrate that the RCAS-mVEGF model can induce new vessel formation in our *ex ova* CAM model.

In vivo mVEGF expression in the *ex ova* CAM model

Clearly, our *in vitro* studies demonstrated that the mVEGF:DF-1 cells produced mVEGF, but we believed

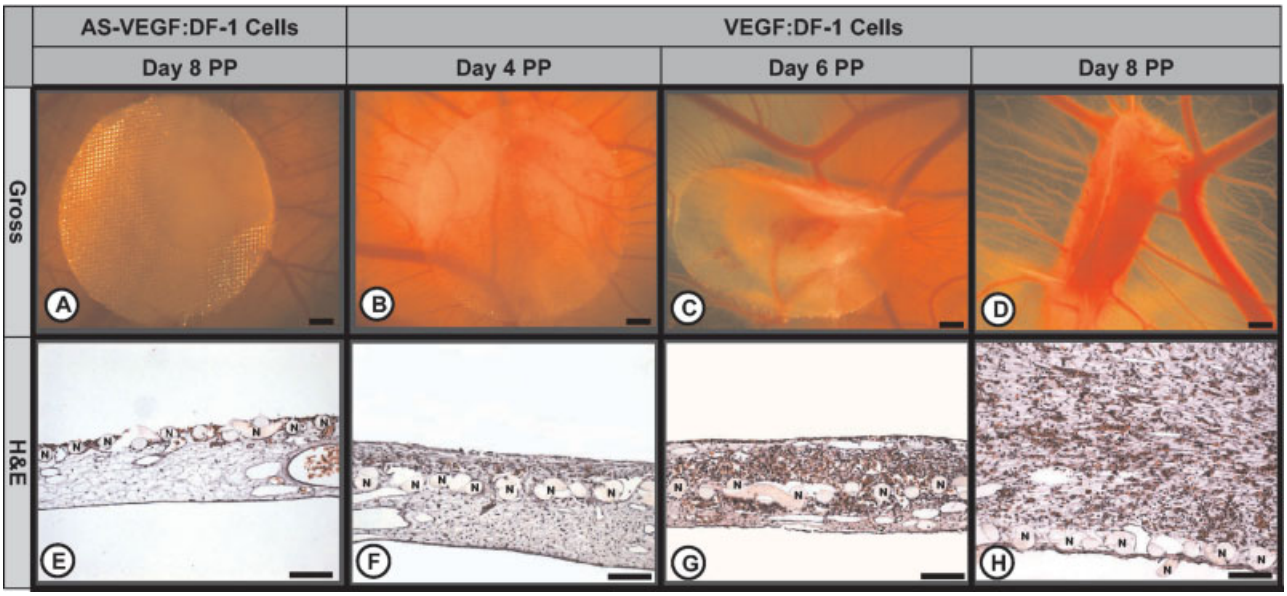

Figure 5. Gross morphological and histological appearance of neovascularization in the *ex ova* CAM model using mVEGF:DF-1 cells grown on nylon disks. Bar size for gross pictures represents 1 mm. Bar size for histology pictures represents 100 μm. [Color figure can be viewed in the online issue, which is available at www.interscience.wiley.com.]

that it was important to demonstrate *in vivo* expression of mVEGF in our CAM model. Analysis of the CAM tissue homogenates demonstrated that CAM tissue from the mVEGF:DF-1–treated CAMs had significant mVEGF content (137.6 ± 3.67 pg of mVEGF per milligram total protein), that none of the CAM tissue from media or control DF-1 cells (DF-1, mVEGF antisense:DF-1 or GFP:DF-1 Cells) had detectable mVEGF in the tissue homogenates. It should be noted that our ELISA detects only mouse VEGF and not chicken VEGF, thus we know that these studies are evaluating only the murine VEGF gene product expressed in DF-1 cells by gene transfer.

Sensor function *in vitro*

Prior to use of our acetaminophen sensor *in vivo*, we evaluated the performance of the sensor *in vitro* (Fig. 8). As a result of our nylon ring data, we chose to design a circular sensor that would act as a "corral" for the mVEGF:DF-1 when added to the sensor placed on the CAM [Fig. 8(A), top view of sensor; Fig. 8(B), side view of sensor]. The acetaminophen sensor performance *in vitro* demonstrated that the sensor showed a dose-dependent response to acetaminophen over a range of 0.5 to 8 m*M* acetaminophen [Fig. 8(C)]. The slope for the response of the acetaminophen sensors was 644 nA/m*M*, with an intercept of 390 nA ($R^2 = 0.988$). The *ex ova* CAM model with an acetaminophen sensor in place at day 9 post–sensor placement is presented in Figure 8(D). These *in vitro* studies demonstrated the functionality and sensitivity of our sensor *in vitro* and thus allowed us to utilize these sensors for our *in vivo* studies, that is, in the *ex ova* CAM model.

Impact of mVEGF gene transfer on sensor function *in vivo*

The focus of these studies was to demonstrate the *in vivo* function of the acetaminophen sensors and to determine the impact of mVEGF-induced increase of vessel density surrounding the sensor on sensor function *in vivo*. In general, sensors were incorporated after only a few days postplacement, and only sensors completely incorporated were finally utilized to compare responses between control sensors and angiogenesis induced around sensor. After 6 days to 10 days PP, sensors were tested using the three-electrode system described in the Methods section above. Sensors implanted on CAMs with buffer or GFP:DF-1 cells displayed no induced neovascularization around the sensor (Fig. 9) and had minimal sensor responses to intravenous acetaminophen injection [i.e., Fig. 10: media, 133.33 ± 27.64 nA ($n = 6$); GFP:DF-1, 187.50 ± 55.43 nA ($n = 6$)]. Alternatively, the sensors implanted with mVEGF:DF-1 cells displayed massive neovascularization (Fig. 9), and equally massive sensor response to intravenously injected acetaminophen [Fig. 10: mVEGF:DF-1, 1387.50 ± 276.42 nA ($n = 6$)]. Statistical analysis indicated that there was no statistical difference in sensor response between media-treated sensors and sensors treated with GFP:DF-1 cells. Alternatively, when the responses of media-treated sensors or GFP:DF-1–treated sensors were compared with

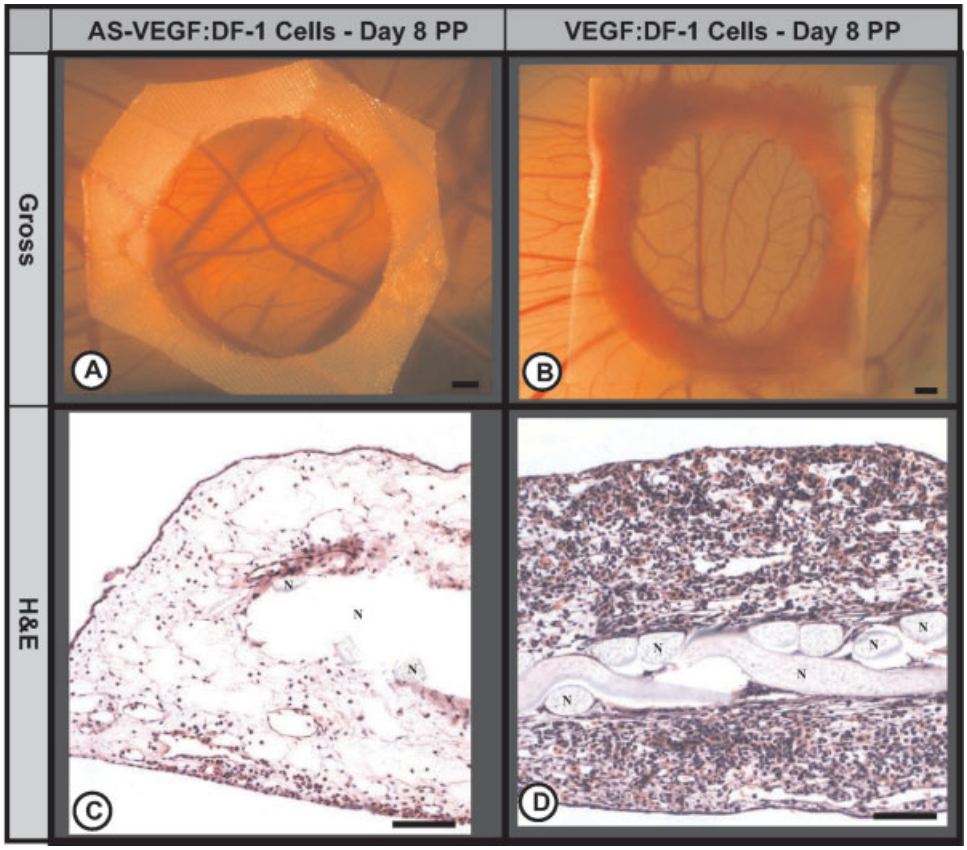

Figure 6. Gross morphological and histological appearance of neovascularization induced in the *ex ova* CAM Model using mVEGF:DF-1 cells added to nylon rings. Bar size for gross pictures represents 1 mm. Bar size for histology pictures represents 100 μm. [Color figure can be viewed in the online issue, which is available at www.interscience.wiley.com.]

mVEGF:DF-1–treated sensors, there was major statistical significance ($p < 0.001$). Finally, when sensor function in the mVEGF:DF-1– and GFP:DF-1–treated sensor-CAM studies were compared over time, the control (GFP:DF-1–treated) sensors were functional at day 4 postimplantation but rapidly lost function by day 6 postimplantation (Fig. 11). This loss of sensor in the *ex ova* CAM model generally paralleled the loss to sensor function seen in a wide variety of mammalian models of implantable sensors. Alternatively, the mVEGF:DF-1–treated sensors were functionally similar to control GFP:DF-1–treated sensors at day 4, but by day 6 PP displayed a massive increase in function that correlated with the appearance of neovascularization around the sensor (Fig. 11). These data clearly support our hypothesis that increased vessel density surrounding a sensor *in vivo* does enhance sensor function *in vivo* and provide "proof of principle" that gene transfer of

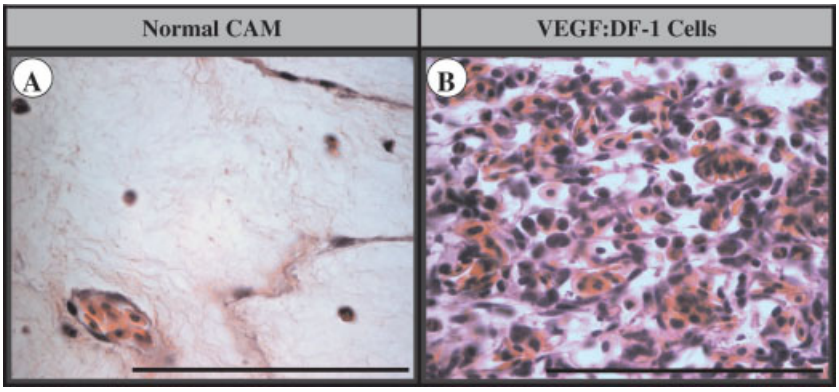

Figure 7. Histological appearance of neovascularization induced in the *ex ova* CAM using mVEGF:DF-1 cells grown on nylon disks. Bar size represents 100 μm. [Color figure can be viewed in the online issue, which is available at www.interscience.wiley.com.]

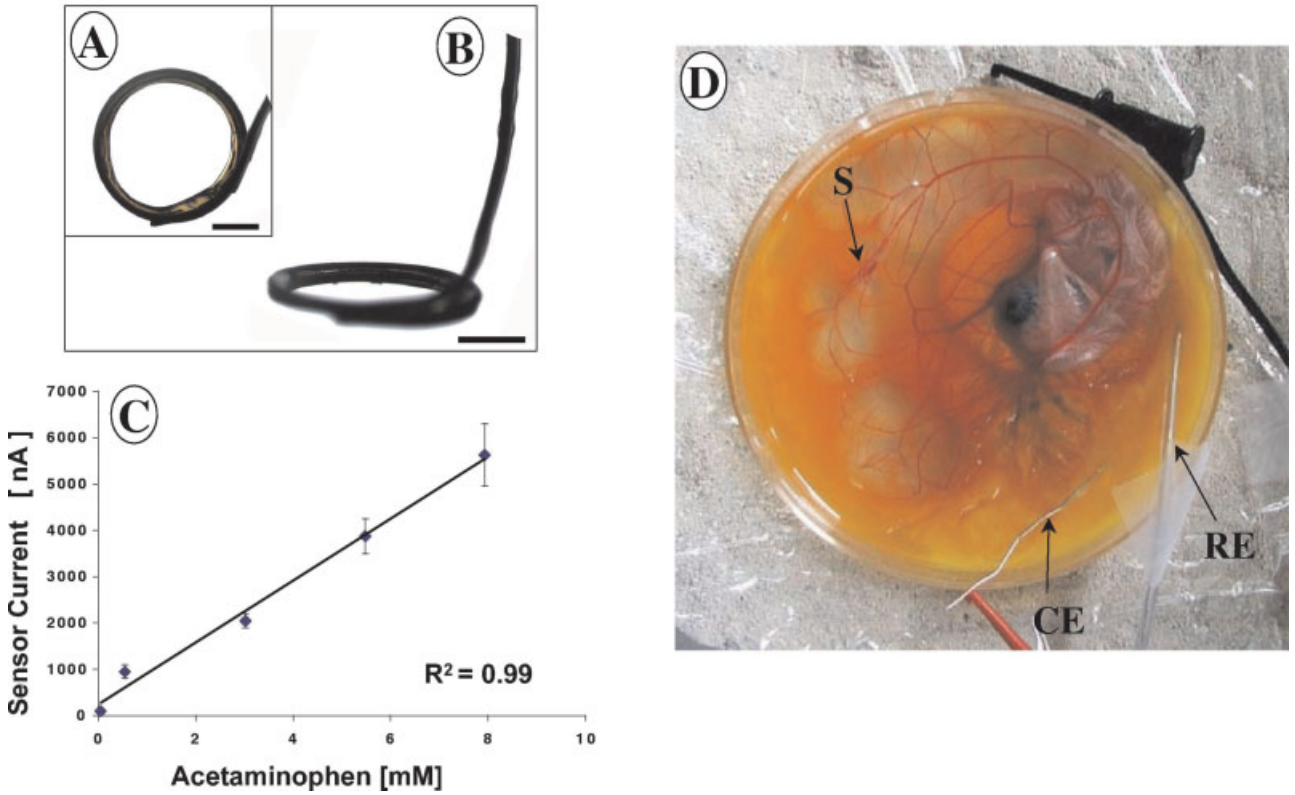

Figure 8. Acetaminophen sensors *in vitro* and *in vivo*. Figure 8(D) sensor (S), reference electrode (RE), and the counter electrodes (CE) are indicated by the arrows. [Color figure can be viewed in the online issue, which is available at www.interscience.wiley.com.]

angiogenic factors such as mVEGF can be used to enhance vessel density around implanted glucose sensors.

DISCUSSION

Sensors and human disease

With the rapid growth in biomedical technology, there has been significant interest in developing implantable biosensors for a wide variety of medical applications. For example, one of the major areas on which the development of effective implantable biosensors would have a major clinical and economic impact is the area of diabetes treatment. It is estimated that 17 million people in the United States have diabetes, with an annual economic cost in the United States of $132 billion.[41] The public health significance of diabetes is manifested in the various long-term complications resulting in premature death, disability, and compromised quality of life, with association of major economic impacts. Currently, the successful management of insulin-dependent diabetes requires monitoring of blood glucose levels by repeatedly obtaining a blood sample from the capillary vasculature ("finger sticks"), with its inherent discomfort and inconvenience. Hence, the development of an implantable glucose sensor is often considered a practical and immediate approach to managing blood glucose levels in diabetics. The relatively slow progress seen in the development of implantable sensors, including the glucose sensor, is caused in large part by the inability to control the complex tissue responses induced by sensor implantation (i.e., inflammation, fibrosis, and loss of vasculature) and by the lack of simple, rapid, and cost-effective *in vivo* models to evaluate sensor function and agents that can control tissue reactions to the implanted sensors (e.g., gene transfer or tissue response modifiers). To begin to overcome these hurdles we have developed a system of genetically engineered cells expressing VEGF, an *ex ova* CAM model, and a simple acetaminophen-based sensor system. Utilizing this system, we demonstrated that VEGF-induced neovascularization around the sensor dramatically enhances sensor function *in vivo*.

Ex ova chick embryo chorioallantoic membrane (CAM) model

One of the major obstacles in developing rationale strategies to control inflammation and fibrosis, surrounding implants such as sensors, is the lack of a

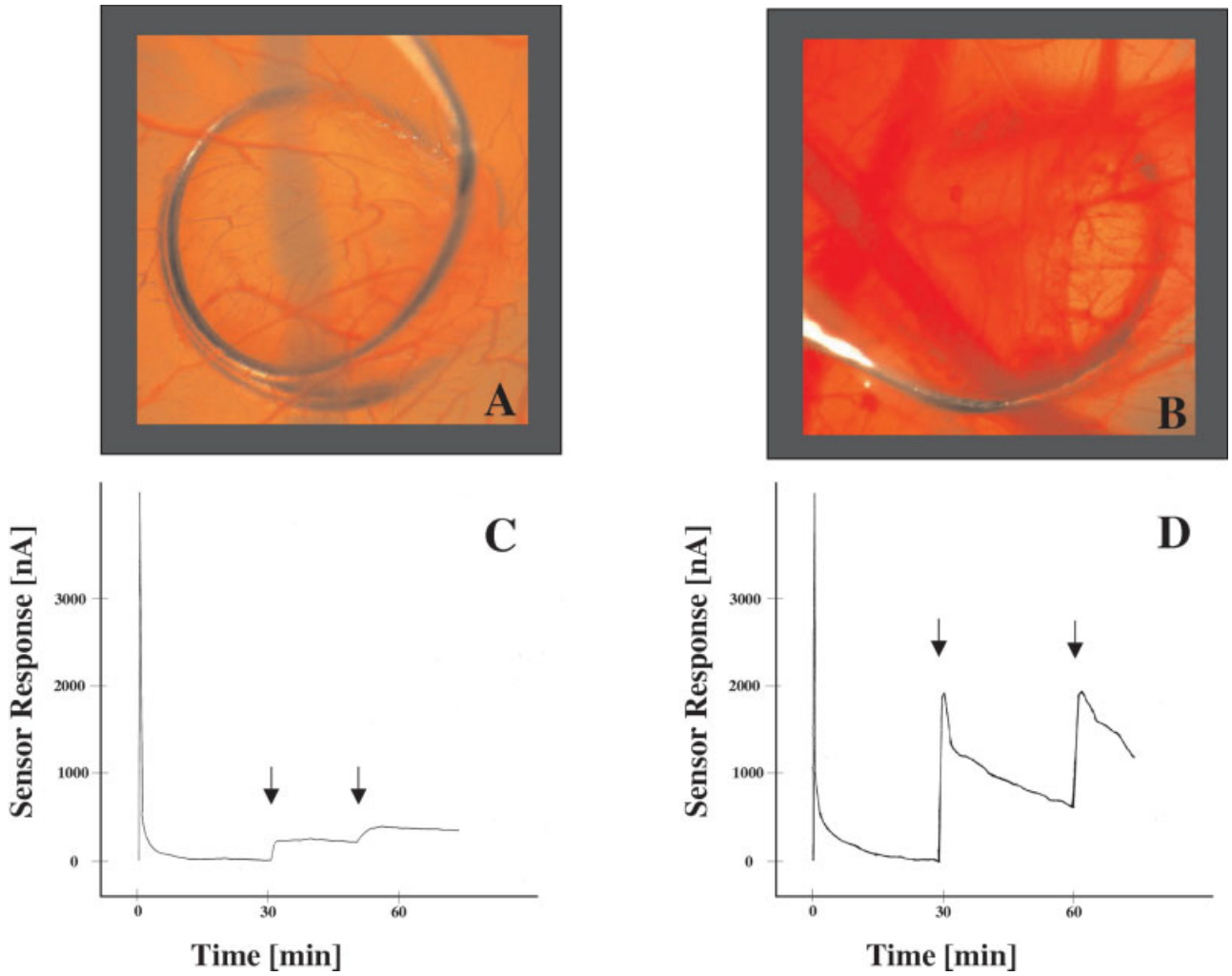

Figure 9. Acetaminophen sensor incorporation and response in the *ex ova* CAM model. Only sensors with mVEGF:DF-1 cells added displayed neovascularization [Fig. 9(B), neither GFP:DF-1, Figure 9(A), nor media-treated sensors (data not shown) displayed any neovascularization on the CAMs. To test sensor function *in vivo*, we injected acetaminophen intravenously into each chick embryo (indicated by the arrows) and determined sensor function as nA response. Injection of acetaminophen caused a minimal response in the GFP:DF-1–treated sensors *in vivo* [Fig. 9(C)]. Media-treated sensors also displayed virtually identical minimal response to intravenous injections of acetaminophen (data not shown). Sensors treated with mVEGF:DF-1 demonstrated a dramatic increase in sensor response [Fig. 9(D)] when compared with the media or GFP:DF-1 cell–treated sensor. [Color figure can be viewed in the online issue, which is available at www.interscience.wiley.com.]

simple and inexpensive *in vivo* model that reacts similarly to mammalian tissue. We recently demonstrated that the *ex ova* model of the chick embryo CAM resembles an excellent model for testing of tissue reaction to biomaterials and implants.[14] The CAM of a developing embryo is a valid alternative to the traditional mammalian models, because it provides a rapid, simple, and low-cost screening of tissue reactions (i.e., acute and chronic inflammation as well as fibrosis) that parallel tissue reactions in mammalian tissues. Additionally, the CAM model has routinely been used to evaluate a wide range of recombinant and naturally occurring angiogenic factors and angiogenesis inhibitors.[23,30,42–44] Thus, the CAM of the chick embryo appears to be a valid *in vivo* model for evaluation of the impact of gene transfer on tissue reactions and sensor function *in vivo*.

Genetically engineered cell systems for delivery of genes *in vitro* and *in vivo*

Our first goal was to develop an effective viral vector system that would promote gene transfer *in vitro* and *in vivo*. In selecting viral vectors for these studies, an important consideration was to have a simple and safe viral vector that could be used safely in large numbers of studies. To this end, we chose a helper-independent retroviral vector, RCAS, for gene transfer in the DF-1

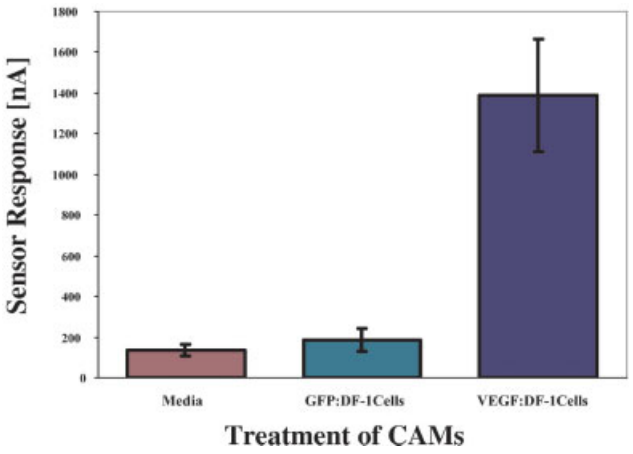

Figure 10. Quantification of the acetaminophen sensor response in the *ex ova* CAM model. [Color figure can be viewed in the online issue, which is available at www.interscience.wiley.com.]

cells and ultimately into the *ex ova* CAM model.[28] This vector system is easily manipulated by standard recombinant DNA methods, it replicates robustly in DF-1 avian cells *in vitro*,[27] and does not infect mammalian cells, which provides an added safety feature.

One of the major problems with viral vector–based gene transfer is that, often, direct placement of the viral vector at the tissue site results in relatively poor virus–gene incorporation. Increasingly, investigators have utilized cell delivery systems to both enhance and sustain local virus/gene production in mammalian systems.[32–35] Our experience in the *ex ova* CAM model was very similar, in that direct placement of only the GFP:RCAS virus on the CAM resulted in few fluorescent cells appearing on the CAM. In parallel studies using mVEGF:RCAS virus only, placement of the virus on the CAM resulted in little to no neovascularization. This may be due to the fact that viruses are very susceptible to drying effects. These observations spurred us to develop and validate a cell-based viral vector delivery system, for example, the GFP:DF-1 and mVEGF:DF-1 cells. We initially utilized the GFP-RCAS system to rapidly evaluate gene transfer protocols. These *in vitro* validated GFP:DF-1 cells were extremely useful in localization and distribution of RCAS:DF-1 cells on the CAMs shortly after transplantation, as well as demonstrating the incorporation of the GFP gene in the CAM cells over time (see Figs. 3 and 4). Using our experience with the GFP:DF-1 cells significantly enhanced the development of the *in vitro* and *in vivo* protocols that made preparing and validating the mVEGF:DF-1 cells much faster and easier. The result of these studies indicated that *in vitro*, the VEGF:DF-1 cell system expressed large amounts of mVEGF and that *in vivo*, the mVEGF:DF-1 cell system produced both expression of VEGF and an extremely explosive neovascularization in the *ex ova* CAM model. We believe that the VEGF expression and extensive neovascularization seen in the mVEGF:DF-1–treated CAM results not only from the mVEGF produced by the original DF-1 cells but also from *in situ* transfection of CAM cells such as tissue fibroblast. Our *in vitro* data clearly demonstrated that virus production parallels mVEGF production in the DF-1 fibroblasts (see Fig. 2), thus supporting the likelihood that the production of virus would expand the number of mVEGF-producing cells in the CAM. Interestingly, the neovascularization seen in the CAM remained localized within the original site of implantation, probably due to the limitations of virus propagation on the CAM, which propagates cell to cell. We noted that there was no difference in the chick development, morbidity, or mortality rates in untreated control chick embryos when compared with embryos treated with media only, DF-1 cells, GFP:DF-1 cells producing GFP and RCAS, or DF-1 cells producing mVEGF and RCAS.

mVEGF:DF-1–induced neovascularization enhances sensor function *in vivo*

The major goals of our *in vivo* studies were to demonstrate not only that we could successfully deliver genes to the chick embryo CAM, thus enhancing neovascularization at sites of sensor implantation, but that this enhanced neovascularization would significantly enhance sensor function *in vivo*. One of the major advantages of the *ex ova* CAM model is that tissue reactions induced in the CAM can be easily and directly visualized, thereby allowing rapid identification

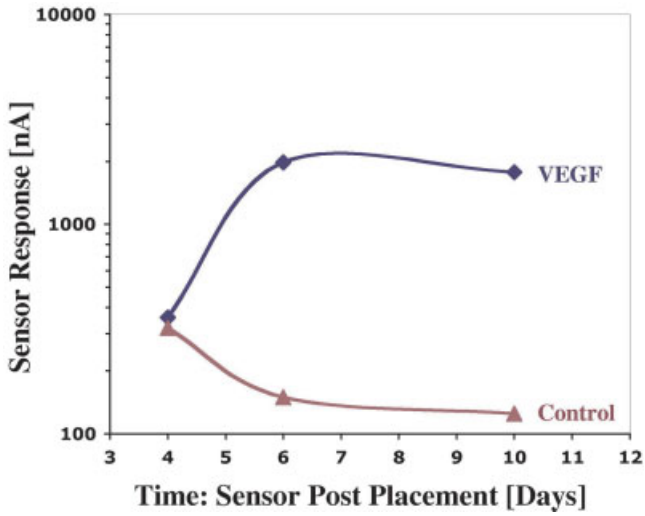

Figure 11. Impact of mVEGF:DF-1 cell–induced neovascularization on the acetaminophen sensor response in the *ex ova* CAM Model. [Color figure can be viewed in the online issue, which is available at www.interscience.wiley.com.]

of the experimental conditions. Direct visualization of neovascularization is not practical in mammalian models because, generally, animal sacrifice and surgical removal of the target tissue must be done to visualize neovascularization *in vivo*.

Although numerous studies have demonstrated that recombinant angiogenic factors can induce short-term (i.e., 24–48 h) angiogenesis in the CAM model, both the literature and our own experience found that unless the recombinant angiogenic factor is continuously applied to the CAM that vessel, regression occurs rapidly.[23,43,45,46] Efforts to utilize various continuous pump systems or daily addition of recombinant angiogenic factors failed to induce or sustain consistent or significant neovascularization in the CAM. It should also be noted that the traditional angiogenesis induced by recombinant angiogenic factor is very superficial in the CAM, involving only the small capillaries associated with the ectodermal epithelial cells and not inducing neovascularization of the full thickness of the CAM, as was seen in the mVEGF:DF-1–treated CAMs. By demonstrating that gene transfer technology could enhance neovascularization around an implanted sensor in our CAM model, thus demonstrating the usefulness of gene transfer, we were able to show the proof of principle that enhanced neovascularization *in vivo* would result in enhanced sensor function *in vivo*. Future studies utilizing other genes in the RCAS system or even other viral vectors can be tested in the CAM system. Additionally, now that we have demonstrated that neovascularization enhances sensor function *in vivo*, efforts to develop vectors and models for mammalian systems can be justified.

We chose the acetaminophen sensor as part of our model system because of its simplicity of design. Because of the simplicity of function, the acetaminophen sensor can function in a wide variety of shapes. We found that our "loop sensor" design provided not only enhanced performance *in vitro*, but *in vivo* the loop sensor allowed for corralling (i.e., localization) of the control of mVEGF:DF-1 cells on the CAM in close proximity of the sensor. Additionally, we found that utilizing a biodegradable matrix (i.e., fibrin) was also key to delivering a large number of cells to the site of sensor implantation. The fact that fibrin is easily biodegradable *in vivo* appears to enhance the timely release of cells to the CAM. Thus, the combination of a loop sensor and a fibrin matrix greatly enhances cell and gene delivery in our CAM model.

Analysis of the sensor response *in vitro* demonstrated that the acetaminophen sensor was very stable *in vitro* and displayed a linear response over 0.5 to 8 m*M* concentrations of acetaminophen. *In vivo*, we found that there was virtually no difference in the sensor response between sensors treated with media (133.33 ± 27.64 nA) or sensors in which control GFP:DF-1 cells (187.50 ± 55.43 nA) were added to the sensors on the CAMs. This is not surprising because we did not see any neovascularization around the media or GFP:DF-1–treated sensors and, therefore, based on our hypothesis, would not expect any enhanced sensor function *in vivo*. We also demonstrated that the VEGF:DF-1 cells not only induce significant neovascularization in the CAM model but that this neovascularization results in a 10-fold increase in the responsiveness of the acetaminophen sensor (1387.50 ± 276.42 nA) when compared with the media-treated sensors, and an increase greater than sevenfold when compared with the GFP:DF-1–treated sensors on the CAMs.

To our knowledge, this is the first demonstration that increased neovascularization around a sensor *in vivo* enhances its function. We believe that these studies provide a foundation and the proof of principle needed to justify further studies to investigate the effectiveness of other angiogenic factors and gene delivery systems, not only in the CAM model but in mammalian models, in the effort to develop effective paradigms, tools that will enhance neovascularization and sensor function in man. This will be extremely important in the development of a long-term glucose sensor for diabetic patients.

CONCLUSION

Our study focuses on developing simple and safe models to develop rapid approaches to control vessel density surrounding an implantable sensor. Using these models and tools, we clearly demonstrated the importance of vessel density on enhancing sensor function *in vivo*. In the future, the same models, genes, technologies, and approaches can be used to provide enhanced function and lifespan of other types of sensors (e.g., glucose sensors) and implants. Thus, the current study validates the *ex ova* chick embryo CAM model as well as RCAS gene transfer technologies as a simple and safe approach to evaluate a wide variety of sensors and provides proof of principle that enhanced blood vessel density around an implantable sensor dramatically enhances sensor function *in vivo*. We also believe that these studies provide new models and approaches for the evaluation and development of a wide range of new molecular tools and strategies to enhance not only biosensor function *in vivo* (e.g., the glucose sensors) but also tissue compatibility for biomaterials and implants.

The authors thank Dr. Kevin Claffey from the University of Connecticut, Farmington, Connecticut, for providing the cDNA for mVEGF.

References

1. Reichert WM, Sharkawy AA. Biosensors. *In:* von Recum AF, editor. Handbook of Biomaterials evaluation. London: Taylor & Francis; 1999. p 439–460.
2. Gerritsen M, Jansen JA, Kros A, Vriezema DM, Sommerdijk NA, Nolte RJ, Lutterman JA, Van Hovell SW, Van der Gaag A. Influence of inflammatory cells and serum on the performance of implantable glucose sensors. J Biomed Mater Res 2001;54:69–75.
3. Gerritsen M, Jansen JA, Lutterman JA. Performance of subcutaneously implanted glucose sensors for continuous monitoring. Neth J Med 1999;54:167–179.
4. Sharkawy AA, Klitzman B, Truskey GA, Reichert WM. Engineering the tissue which encapsulates subcutaneous implants. I. Diffusion properties. J Biomed Mater Res 1997;37:401–412.
5. Sharkawy AA, Klitzman B, Truskey GA, Reichert WM. Engineering the tissue which encapsulates subcutaneous implants. II. Plasma–tissue exchange properties. J Biomed Mater Res 1998; 40:586–597.
6. Sharkawy AA, Klitzman B, Truskey GA, Reichert WM. Engineering the tissue which encapsulates subcutaneous implants. III. Effective tissue response times. J Biomed Mater Res 1998;40: 598–605.
7. Kornowski R, Fuchs S, Leon MB, Epstein SE. Delivery strategies to achieve therapeutic myocardial angiogenesis. Circulation 2000;101:454–458.
8. Lee SH, Wolf PL, Escudero R, Deutsch R, Jamieson SW, Thistlethwaite PA. Early expression of angiogenesis factors in acute myocardial ischemia and infarction [see comments]. N Engl J Med 2000;342:626–633.
9. Levy AP, Levy NS, Loscalzo J, Calderone A, Takahashi N, Yeo KT, Koren G, Colucci WS, Goldberg MA. Regulation of vascular endothelial growth factor in cardiac myocytes. Circ Res 1995;76: 758–766.
10. Losordo DW, Vale PR, Symes JF, Dunnington CH, Esakof DD, Maysky M, Ashare AB, Lathi K, Isner JM. Gene therapy for myocardial angiogenesis: initial clinical results with direct myocardial injection of phVEGF165 as sole therapy for myocardial ischemia. Circulation 1998;98:2800–2804.
11. Losordo DW, Vale PR, Isner JM. Gene therapy for myocardial angiogenesis. Am Heart J 1999;138:S132–S141.
12. Patel SR, Lee LY, Mack CA, Polce DR, El-Sawy T, Hackett NR, Ilercil A, Jones EC, Hahn RT, Isom OW, Rosengart TK, Crystal RG. Safety of direct myocardial administration of an adenovirus vector encoding vascular endothelial growth factor 121. Hum Gene Ther 1999;10:1331–1348.
13. Rosengart TK, Lee LY, Patel SR, Sanborn TA, Parikh M, Bergman GW, Hachamovitch R, Szulc M, Kligfield PD, Okin PM, Hahn RT, Devereux RB, Post MR, Hackett NR, Foster T, Grasso TM, Lesser ML, Isom OW, Crystal RG. Angiogenesis gene therapy: phase I assessment of direct intramyocardial administration of an adenovirus vector expressing VEGF121 cDNA to individuals with clinically significant severe coronary artery disease. Circulation 1999;100:468–474.
14. Klueh U, Moussy F, Dorsky D, Kreutzer DL. *Ex ova* chick chorioallantoic membrane (CAM) as a novel model for evaluation of tissue responses to biomaterials and implants. J Biomed Mater Res. Forthcoming.
15. Iruela-Arispe ML, Lombardo M, Krutzsch HC, Lawler J, Roberts DD. Inhibition of angiogenesis by thrombospondin-1 is mediated by 2 independent regions within the type 1 repeats. Circulation 1999;100:1423–1431.
16. Gogate SS, Gupta NP, Molherkar L. Effect of different viruses on early development of chick embryo cultured *in vitro*. Indian J Med Res 1979;70:525–528.
17. Hamamichi S, Nishigori H. Establishment of a chick embryo shell-less culture system and its use to observe change in behavior caused by nicotine and substances from cigarette smoke. Toxicol Lett 2001;119:95–102.
18. Thompson J, Bannigan J. Effects of cadmium on formation of the ventral body wall in chick embryos and their prevention by zinc pretreatment. Teratology 2001;64:87–97.
19. Tomanek RJ, Schatteman GC. Angiogenesis: new insights and therapeutic potential. Anat Rec 2000;261:126–135.
20. Yancopoulos GD, Davis S, Gale NW, Rudge JS, Wiegand SJ, Holash J. Vascular-specific growth factors and blood vessel formation. Nature 2000;407:242–248.
21. Leung DW, Cachianes G, Kuang WJ, Goeddel DV, Ferrara N. Vascular endothelial growth factor is a secreted angiogenic mitogen. Science 1989;246:1306–1309.
22. Ferrara N. Molecular and biological properties of vascular endothelial growth factor. J Mol Med 1999;77:527–543.
23. Jiang BH, Zheng JZ, Aoki M, Vogt PK. Phosphatidylinositol 3-kinase signaling mediates angiogenesis and expression of vascular endothelial growth factor in endothelial cells. Proc Natl Acad Sci USA 2000;97:1749–1753.
24. Flamme I, Breier G, Risau W. Vascular endothelial growth factor (VEGF) and VEGF receptor 2 (flk-1) are expressed during vasculogenesis and vascular differentiation in the quail embryo. Dev Biol 1995;169:699–712.
25. Flamme I, von Reutern M, Drexler HC, Syed-Ali S, Risau W. Overexpression of vascular endothelial growth factor in the avian embryo induces hypervascularization and increased vascular permeability without alterations of embryonic pattern formation. Dev Biol 1995;171:399–414.
26. Schaefer-Klein J, Givol I, Barsov EV, Whitcomb JM, VanBrocklin M, Foster DN, Federspiel MJ, Hughes SH. The EV-O–derived cell line DF-1 supports the efficient replication of avian leukosis-sarcoma viruses and vectors. Virology 1998; 248:305–311.
27. Himly M, Foster DN, Bottoli I, Iacovoni JS, Vogt PK. The DF-1 chicken fibroblast cell line: transformation induced by diverse oncogenes and cell death resulting from infection by avian leukosis viruses. Virology 1998;248:295–304.
28. Hughes SH, Greenhouse JJ, Petropoulos CJ, Sutrave P. Adaptor plasmids simplify the insertion of foreign DNA into helper-independent retroviral vectors. J Virol 1987;61:3004–3012.
29. Sambrook J, Fritsch EF, Maniatis T. Molecular cloning. NY: Cold Spring Harbor Press; 1989.
30. Ribatti D, Vacca A. Models for studying angiogenesis *in vivo*. Int J Biol Markers 1999;14:207–213.
31. Schmidt M, Flamme I. The *in vivo* activity of vascular endothelial growth factor isoforms in the avian embryo. Growth Factors 1998;15:183–197.
32. Zeng G, Gao L, Birkle S, Yu RK. Suppression of ganglioside GD3 expression in a rat F-11 tumor cell line reduces tumor growth, angiogenesis, and vascular endothelial growth factor production. Cancer Res 2000;60:6670–6676.
33. Oku T, Tjuvajev JG, Miyagawa T, Sasajima T, Joshi A, Joshi R, Finn R, Claffey KP, Blasberg RG. Tumor growth modulation by sense and antisense vascular endothelial growth factor gene expression: effects on angiogenesis, vascular permeability, blood volume, blood flow, fluorodeoxyglucose uptake, and proliferation of human melanoma intracerebral xenografts. Cancer Res 1998;58:4185–4192.
34. Claffey KP, Brown LF, del Aguila LF, Tognazzi K, Yeo KT, Manseau EJ, Dvorak HF. Expression of vascular permeability factor/vascular endothelial growth factor by melanoma cells increases tumor growth, angiogenesis, and experimental metastasis. Cancer Res 1996;56:172–181.
35. Leenders W, van Altena M, Lubsen N, Ruiter D, De Waal R. In vivo activities of mutants of vascular endothelial growth factor (VEGF) with differential *in vitro* activities. Int J Cancer 2001;91: 327–333.

36. Malitesta C, Palmisano F, Torsi L, Zambonin PG. Glucose fast-response amperometric sensor based on glucose oxidase immobilized in an electropolymerized poly(o-phenylenediamine) film. Anal Chem 1990;62:2735–2740.
37. Moussy F, Harrison DJ, O'Brien DW, Rajotte RV. Performance of subcutaneously implanted needle-type glucose sensors employing a novel trilayer coating. Anal Chem 1993;65:2072–2077.
38. Moussy F, Jakeway S, Harrison DJ, Rajotte RV. In vitro and in vivo performance and lifetime of perfluorinated ionomer–coated glucose sensors after high temperature curing. Anal Chem 1994;66:3882–3888.
39. Moatti-Sirat D, Poitout V, Thome V, Gangnerau MN, Zhang Y, Hu Y, Wilson GS, Lemonnier F, Klein JC, Reach G. Reduction of acetaminophen interference in glucose sensors by a composite Nafion membrane: demonstration in rats and man. Diabetologia 1994;37:610–616.
40. Valdes TI, Kreutzer D, Moussy F. The chick chorioallantoic membrane as a novel *in vivo* model for the testing of biomaterials. J Biomed Mater Res 2002;62:273–282.
41. ADA American Diabetes Association–Basic Diabetes Information. http://www.diabetes.org/main/application/commercewf; 2002.
42. Kessler DA, Langer RS, Pless NA, Folkman J. Mast cells and tumor angiogenesis. Int J Cancer 1976;18:703–709.
43. Oh SJ, Jeltsch MM, Birkenhager R, McCarthy JE, Weich HA, Christ B, Alitalo K, Wilting J. VEGF and VEGF-C: specific induction of angiogenesis and lymphangiogenesis in the differentiated avian chorioallantoic membrane. Dev Biol 1997;188:96–109.
44. Ribatti D, Vacca A, Roncali L, Dammacco F. The chick embryo chorioallantoic membrane as a model for *in vivo* research on angiogenesis. Int J Dev Biol 1996;40:1189–1197.
45. Dallabrida SM, De Sousa MA, Farrell DH. Expression of antisense to integrin subunit beta 3 inhibits microvascular endothelial cell capillary tube formation in fibrin. J Biol Chem 2000;275:32281–32288.
46. Wilting J, Christ B, Bokeloh M, Weich HA. In vivo effects of vascular endothelial growth factor on the chicken chorioallantoic membrane. Cell Tissue Res 1993;274:163–172.